

## A High Rate Zinc/MCM-41/Air Cell

Hens Saputra<sup>1</sup> and Raihan Othman<sup>2\*</sup>

<sup>1</sup>Pusat Teknologi Industri Proses  
Badan Pengkajian dan Penerapan Teknologi (BPPT)

Jl. M.H. Thamrin No. 8  
Jakarta 10340, Indonesia

<sup>2</sup>Faculty of Engineering  
International Islamic University Malaysia

P.O. Box 10  
50728 Kuala Lumpur, Malaysia

\*Corresponding author  
Phone: +60-3-61964561  
Fax: +60-3-61964853  
Email: raihan@iium.edu.my

### Abstract

We report the performance characteristics of a high discharge rate zinc-air cell, assembled in compact, monopolar and bipolar configurations. The use of inorganic MCM-41 membrane enables the construction of a thin, compact cell design with ease. MCM-41 consists of a hexagonally-ordered nanopore structure and is characterized by its large surface area and pore volume, very narrow pore size distribution, hydrophilic in nature and very good thermal stability. The monopolar Zinc/MCM-41/air cell demonstrates discharge charac-

teristics of comparable performance to commercial cells. The cell, 1 cm<sup>2</sup> area x ca. 460 μm thick, possesses limiting current of 27 mA, maximum power output of 31 mW, and volumetric energy density of 924 Wh l<sup>-1</sup>, rated at 20 mA. A bipolar design markedly improves the cell performance. The cell, 1 cm<sup>2</sup> area x ca. 920 μm thick, possesses limiting current of 95 mA, maximum power output of 107 mW, and volumetric energy density of 1189 Wh l<sup>-1</sup>.

**Keywords:** Bipolar design; Inorganic separator; MCM-41 membrane; Zinc-air cell.

### 1. Introduction

Since Smee (1840) first described a primary, acidic zinc-air cell in the literature, the zinc-air electrochemical systems have been extensively studied and developed (Backhurst *et al.*, 1996; Chakkaravarthy *et al.*, 1981; Dewi *et al.*, 2003; Ghiurcan *et al.*, 2003; Goldstein *et al.*, 1999; Jiricny *et al.*, 2000; Muller *et al.*, 1998; Othman *et al.*, 2002; Saputra *et al.*, 2011; Savaskan *et al.*, 1992; Zhang and Zhang, 2004). Popularly dubbed as breathing batteries, zinc-air cells or metal-air batteries in general are unique in that they utilize oxygen from the ambient air as one of the electroactive materials. Hence this provides them with practically unlimited and free oxygen supply. Further, the use of atmospheric oxygen does not require storage, which in principle reduces the weight and simplifies the battery design. Consequently, the metal active material can accommodate the whole compartment

producing a high energy density battery.

Recently, we introduced inorganic MCM-41 membrane as a new separator material for electrochemical cells and demonstrated its efficacy in alkaline zinc-air cell (Saputra *et al.*, 2011). MCM-41 material belongs to a group of mesoporous materials known as M41S, first discovered by researchers of the Mobil Research and Development Corporation in 1992 (Beck *et al.*, 1992; Kresge *et al.*, 1992). This class of material possesses regular arrays of uniform channels with large surface area and is tuneable between 1 nm to 10 nm or more, depending on the choice of surfactant, auxiliary chemicals and reaction conditions (Øye *et al.*, 2001).

The use of MCM-41 membrane separator is attractive due to its 3-in-1 functional features i.e. serving as an electronically insulating separator, ionically conducting membrane and electrolyte storage, simultaneously. The

customary polymer based separators are hydrophobic in nature, thus require an additional absorbent interseparator material as the electrolyte reservoir, particularly for compact cell design. Furthermore, the fabrication of MCM-41 membrane is simply by dip-coating procedure. As a result, the membrane separator could be designed to be sufficiently thin and the construction of bipolar cell configuration could be done with ease. In the present work, we report the fabrication and performance characteristics of bipolar Zn/MCM-41/air cell. The positive attributes of MCM-41 membrane separator as mentioned above resulted in a high rate capacity cell which is of comparable performance with commercial zinc-air cell, if not better.

## 2. Materials and Methods

### 2.1 Preparation of MCM-41 membrane

MCM-41 membrane was fabricated onto the zinc anode substrate using the dip-coating technique. The parent solution for synthesis consisted of quarternary ammonium surfactant, cethyltrimethylammonium bromide  $C_{16}H_{33}(CH_3)_3NBr$  (CTAB), hydrochloric acid, deionized water, ethanol, and tetraethylortosilicate (TEOS) with molar ratio formulation of 0.05 CTAB, 1.0 TEOS, 0.5 HCl, 25  $C_2H_5OH$  and 75  $H_2O$ . After the parent solution was stirred for an hour (about 200 rpm) at room temperature of  $30^\circ C$ , the zinc substrate was dipped into the parent solution and then air dried. A one-time dipping process normally resulted in MCM-41 film thickness of ca.  $1 \mu m$  (Jia *et al.*, 2004; Sano *et al.*, 1997). We applied three times dipping procedure to ensure that the mem-

brane would be thick enough to avoid defects such as cracking and pinhole.

### 2.2 Characterization of MCM-41 membrane

The structural formation of MCM-41 membrane onto the zinc substrate was verified using X-ray diffraction (Cu  $K\alpha$  radiation, a scan range of 1 - 8 degrees of  $2\theta$  and a scan speed of  $2^\circ \text{ min}^{-1}$ ). Its surface morphology was observed using an Atomic Force Microscopy (AFM).

### 2.3 Zinc-air cell components and fabrication

#### 2.3.1 Zinc anode

Zinc anode was prepared from an electrodeposition process in order to obtain a high purity active material with high surface area. An acidic chloride plating bath was utilized. The electrolytic cell consisted of zinc foil (99.9 % purity) as the working electrode and copper foil as the counter electrode-cum-substrate. The copper substrate was clamped by a home-made acrylic board holder. The cell holder served to fix the electrode spacing and to define the deposition area. The electrode spacing was fixed at 30 mm and the holder possessed a window of 1 cm x 1 cm square area for zinc deposition. The electrolyte consisted of zinc chloride (2 M) as the metal source and ammonium chloride (2 M) as the supporting electrolyte. Deposition current density was fixed at  $100 \text{ mA cm}^{-2}$  for a duration of 1.5 hours. The electrodeposition set up and parameters were adopted from the work of Nor Hairin (2011). The resulting zinc deposits weighed 0.35 g and ca.  $100 \mu m$  thick. *Figure 1* compares the surface mor-

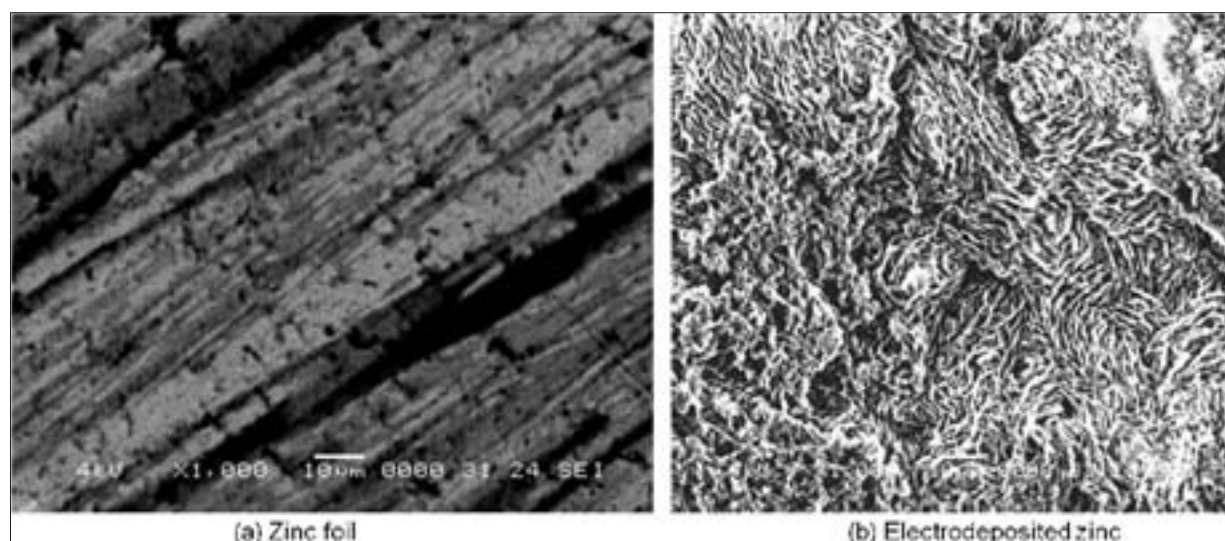


*Figure 1.* SEM micrographs indicating the high surface area obtained from electrodeposited zinc as compared to compact zinc foil.

phology images between a compact zinc foil and the electrodeposited zinc. It clearly signifies the high surface area advantage of the zinc electrodeposits. The images were observed using Field-Emission Scanning Electron Microscope (FE-SEM) (JED-2100, JEOL Co. Ltd.). Nor Hairin (2011) reported that zinc electrodeposits prepared from the set up described above possessed specific surface area in excess of  $300 \text{ m}^2 \text{ g}^{-1}$  and porosity of 62 %.

### 2.3.2 Air cathode

A commercially available air cathode sheet (ca.  $350 \mu\text{m}$  thick) was utilized. The air cathode consisted of laminated structures of fibrous carbon supported by a nickel mesh and the air-side of the electrode covered with a gas permeable, hydrophobic, Teflon layer. The membrane permits ambient air oxygen to diffuse into the system. The Teflon hydrophobic characteristic maintains the crucial triple interface (air/oxygen-liquid/ electrolyte-solid/conductor) requirement for an effective functioning of the air electrode (Chakkaravarthy *et al.*, 1981).

### 2.3.3 Separator and electrolyte

MCM-41 membrane, prepared onto the zinc anode substrate, served as the cell's separator as well as the

electrolyte storage due to its hydrophilic characteristic. An aqueous KOH electrolyte (6 M) was utilized. The main issue concerning the use of MCM-41 membrane separator in caustic alkaline environment is its stability since it is a silica-based structure. However, we discovered that the material is tolerable up to 70 % of KOH weight ratio content without adversely causing electrochemical cell failure or short circuiting (Saputra *et al.*, 2012). The ordered silica network only diminished when the KOH content reached 80 wt. %. The KOH weight ratio content was calculated from the following relation

$$\text{wt. \%} = \frac{W_{\text{KOH(aq)}}}{W_{\text{KOH(aq)}} + W_{\text{MCM-41}}} \times 100\% \quad (1)$$

where  $W_{\text{KOH(aq)}}$  and  $W_{\text{MCM-41}}$  denote the weight of aqueous KOH electrolyte and MCM-41 material respectively.

### 2.3.4 Cell design

The planar structure of monopolar cell design is depicted in *Figure 2*. The cell dimension was ca.  $1 \text{ cm}^2$  area x ca.  $460 \mu\text{m}$  thick. The bipolar cell design was assembled from positives consisting of two single air electrodes facing back to back, and a single negative placed in between. The negative electrode comprised of

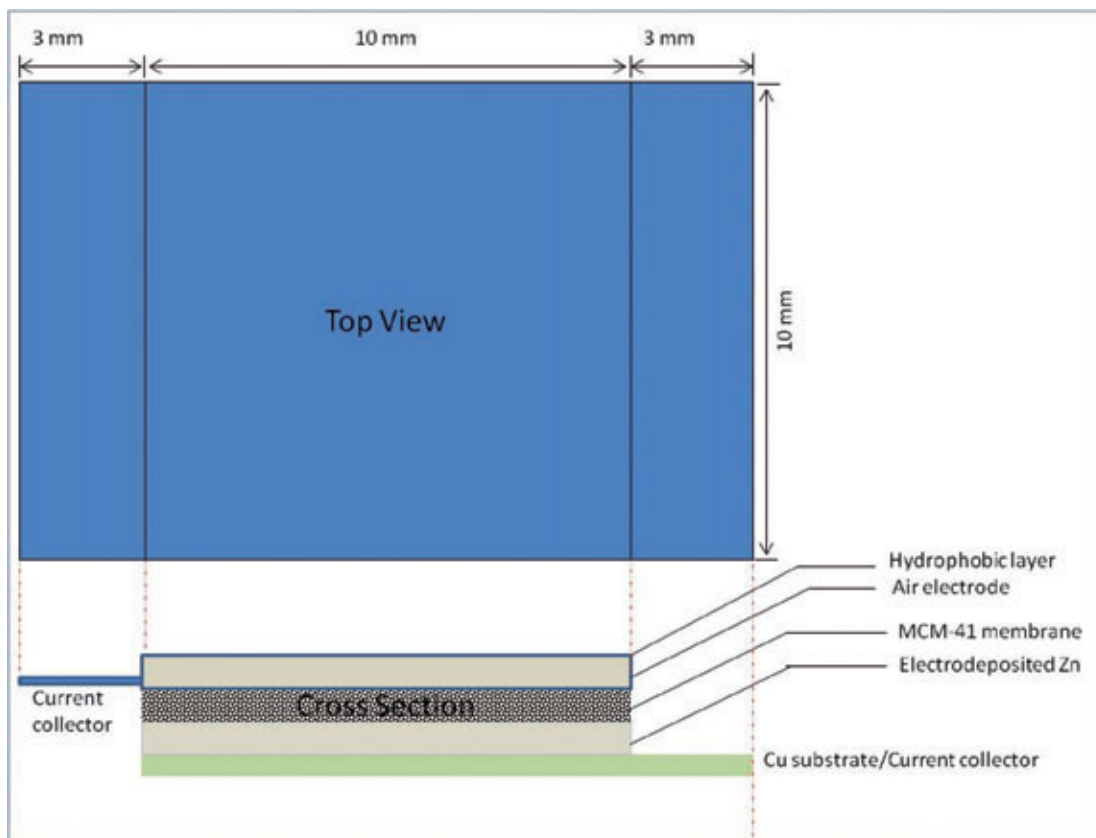


*Figure 2.* Schematic illustration of monopolar Zn/MCM-41/air cell.

electroplated zinc on both sides of the copper substrate and coated with MCM-41 membrane. The cell dimension was 1 cm<sup>2</sup> area x ca. 920 μm thick. **Figure 3** illustrates the bipolar cell configuration.

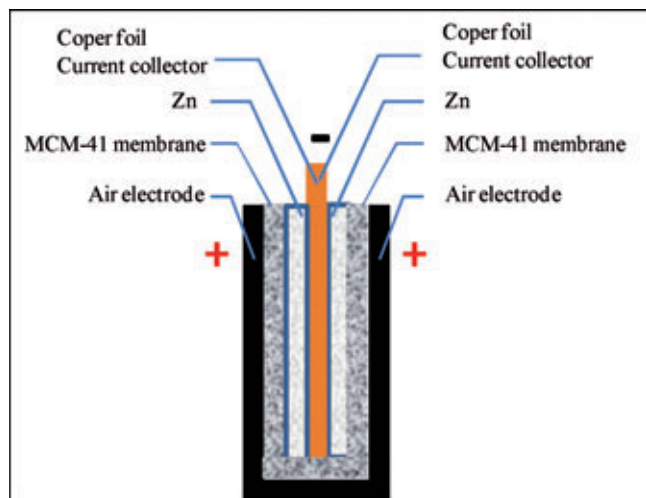


**Figure 3.** Bipolar Zn/MCM-41/air cell configuration

## 2.4 Cell characterizations

The assembled cells were characterized according to their open circuit potential (OCV), polarization curve, power density profile and discharge capacity. An Eco Chemie (The Netherland) Autolab Galvanostat/ Potentiostat was utilized to perform the measurements. The characterizations were conducted at ambient room temperature.

A polarization profile is essentially a V-I plot i.e. the variation of operating voltage as a function of discharge current. Power density plot can be subsequently obtained by measuring the cell power output, P (product of V and I) at each particular discharge current. Based on the P-I plot, the maximum power that the cell could deliver is readily obtained.

Cell discharge capacity is a measure of total charge quantity that an electrochemical cell could supply. In this work, we adopted a galvanostatic discharge test.

## 3. Results and Discussion

MCM-41 mesoporous structure is constructed from cationic surfactant, cetyltrimethyl-ammonium bromide (CTAB), and the resulting organic template finally covered by silica from tetraethylorthosilicate (TEOS). The transition between different forms of aggregates is determined by the critical micelle concentration (CMC).

Since there are more than one, transition occurs over the concentration spectrum, the CMC at lowest concentration is designated as CMC1 and the subsequent CMCs designated as CMC2, CMC3 and so on. At very low concentration, the surfactant molecules are randomly dispersed in solution. As the concentration reaches CMC1, spherical micelles are formed in which the outer surface comprised of the hydrophilic heads of surfactant molecules, while the tails of these molecules are directed toward the centre of the sphere. Increase of concentration to CMC2 causes a transition from the spherical micelles to more elongated or rod-like micelles. Further increase in concentration causes the orientation and close packing of the elongated micelles into hexagonal arrays of MCM-41 structure. This is the liquid crystalline state termed as the middle phase or hexagonal phase (Lee and Rathman, 2001).

The pore size of MCM-41 structure varies between 1-10 nm and is determined by the length of carbon chain of CTAB cationic surfactant (Saputra, 2003; Kresge *et al.*, 1992; Øye *et al.*, 2001). Repeated measurements from our earlier work have ascertained that the as-synthesized MCM-41 material possessed a narrow pore size distribution which centred around 2 nm, BET (Brunauer-Emmett-Teller) surface area of 1200 m<sup>2</sup> g<sup>-1</sup>, and pore volume density of 1.08 cm<sup>3</sup> g<sup>-1</sup> (Saputra, 2003; Saputra *et al.*, 2011a). The pore surface of MCM-41 is covered by silanol groups (Si-OH) formed during the synthesis of the material. The density of silanol groups is around 2.5-5 nm<sup>2</sup> and very much depends on the template removal conditions (Chen *et al.*, 1996). The silanol group, in particular the Q<sup>3</sup> group ((SiO)<sub>3</sub>Si-OH), serves as hydration site (Zhao *et al.*, 1998). The hydrophilic characteristic of MCM-41 material is attributed to the existence of this type of silanol group which forms around 60-80 % of the silanol group.

MCM-41 hexagonal lattice structure is characterized by low angle X-ray diffraction peaks as listed in Table 1 (Kresge *et al.*, 1992; Øye *et al.*, 2001). The dominant (100) diffraction ( $2\theta \approx 2^\circ$ ) normally suppressed the remaining peaks (Jia *et al.*, 2004). **Figure 4** depicts the X-ray diffractogram of the as-synthesized MCM-41 material which confirms its structural formation. The AFM topography image of **Figure 5** reveals the high surface area nature of the membrane.



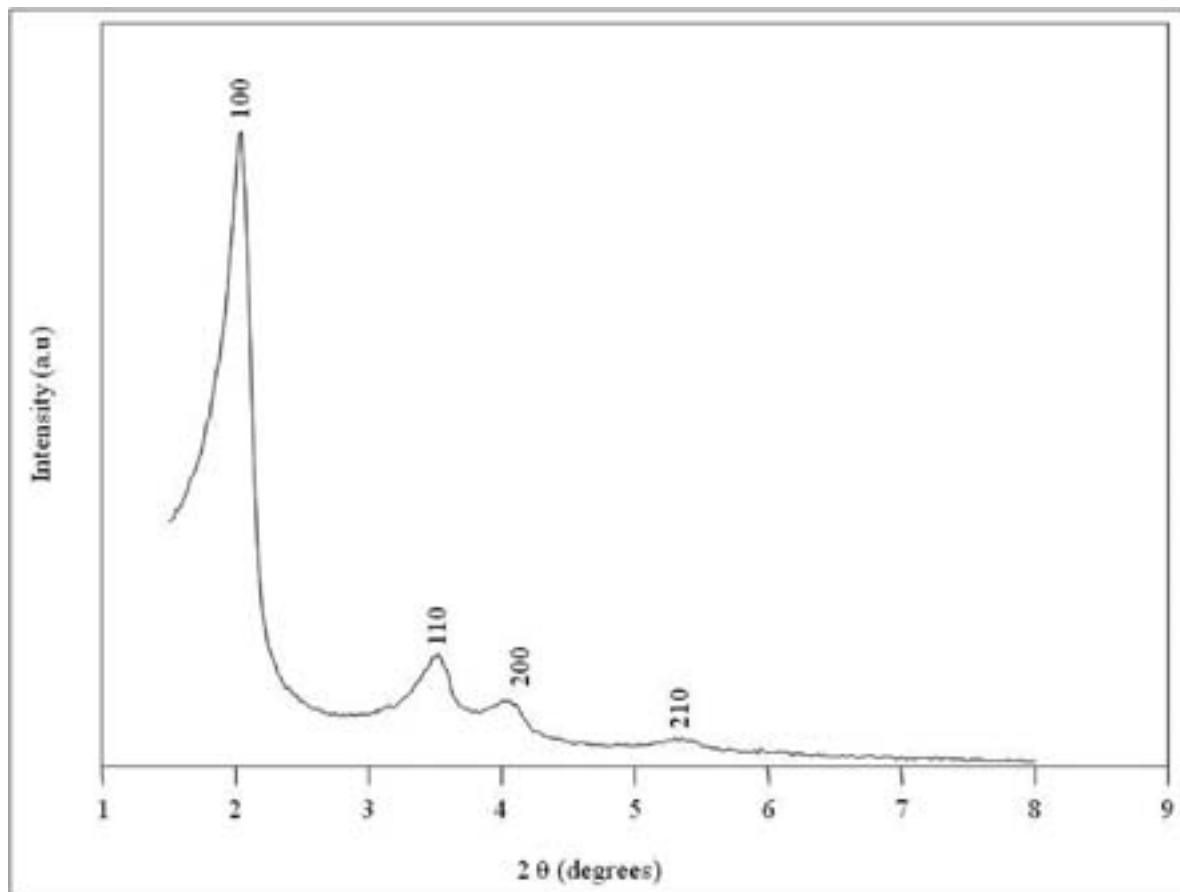


Figure 4. X-Ray diffractogram of the as-synthesized MCM-41 confirming the existence of hexagonal lattice structure.

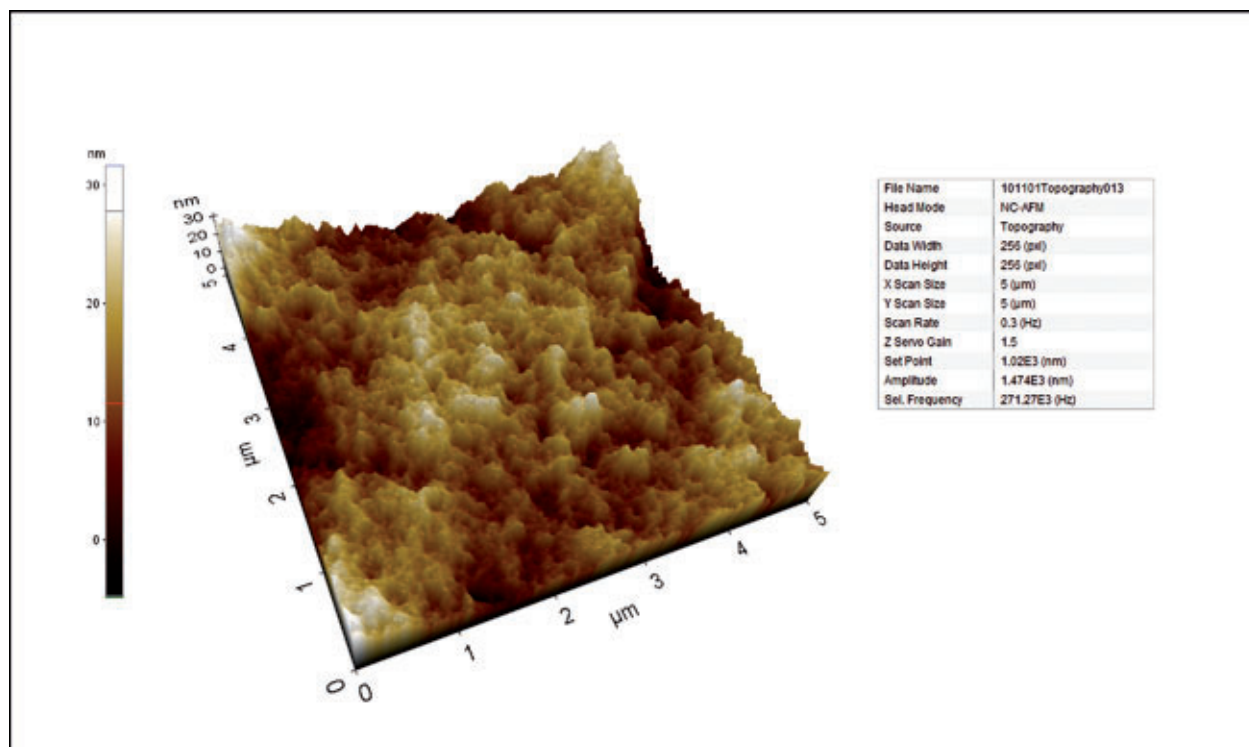


Figure 5. AFM surface topology image of the MCM-41 membrane.

**TABLE 1. Characteristic of MCM-41 X-ray diffractogram.**

<i>hkl</i>	<i>d</i> /Å
100	39.8
110	22.9
200	19.8
210	14.9

The fabricated Zn/MCM-41/air cells registered a stable open circuit voltage (OCV) value of 1.5 V. *Figure 6* displays the profile of operating voltage as a function of discharge current, for both cell configurations. Bipolar cell configuration possesses better polarization profile. The improvement in the operating voltage as a result of bipolar design was approximately 10 % in average, i.e. around 120 mV. The enhancement in the cell's limiting current for bipolar design was even more substantial. Limiting current is the highest load current of which the cell is capable to deliver prior to the abrupt drop in the operating voltage. Monopolar cell was capable

to deliver at most 27 mA, but for bipolar cell the limiting current was extended almost to an order of magnitude of 95 mA. *Figure 7* depicts the performance comparison in term of power output. As the power output is obtained from the product of operating voltage and load current, the difference between the two profiles are more prominent. Monopolar cell registered a maximum power output of 31 mW at load current of 27 mA while the bipolar cell delivered a maximum power output of 107 mW at load current at 95 mA, i.e. more than threefold enhancement.

Discharge capacity of an electrochemical cell is an empirical quantity which is a function of discharge current. In order to obtain an optimum cell capacity, the monopolar cell was subjected to various discharge currents. *Table 2* below highlights the cell discharge characteristics obtained at load current of 10 mA, 15 mA, 20 mA and 30 mA. Obviously, optimum cell performance was obtained at load current of 20 mA i.e. based on the cell capacity and total energy output.

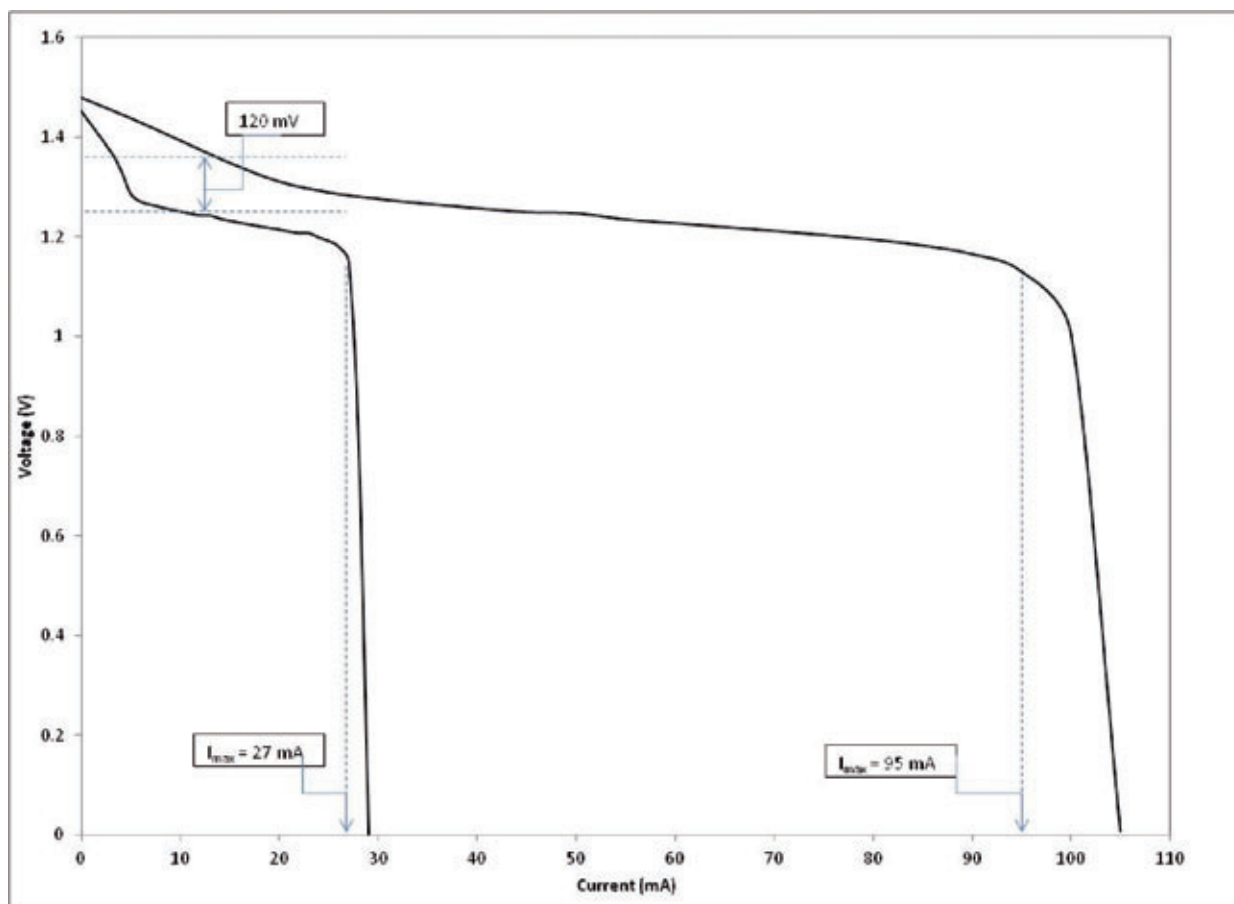


*Figure 6. Polarization profiles of monopolar and bipolar cell configurations.*

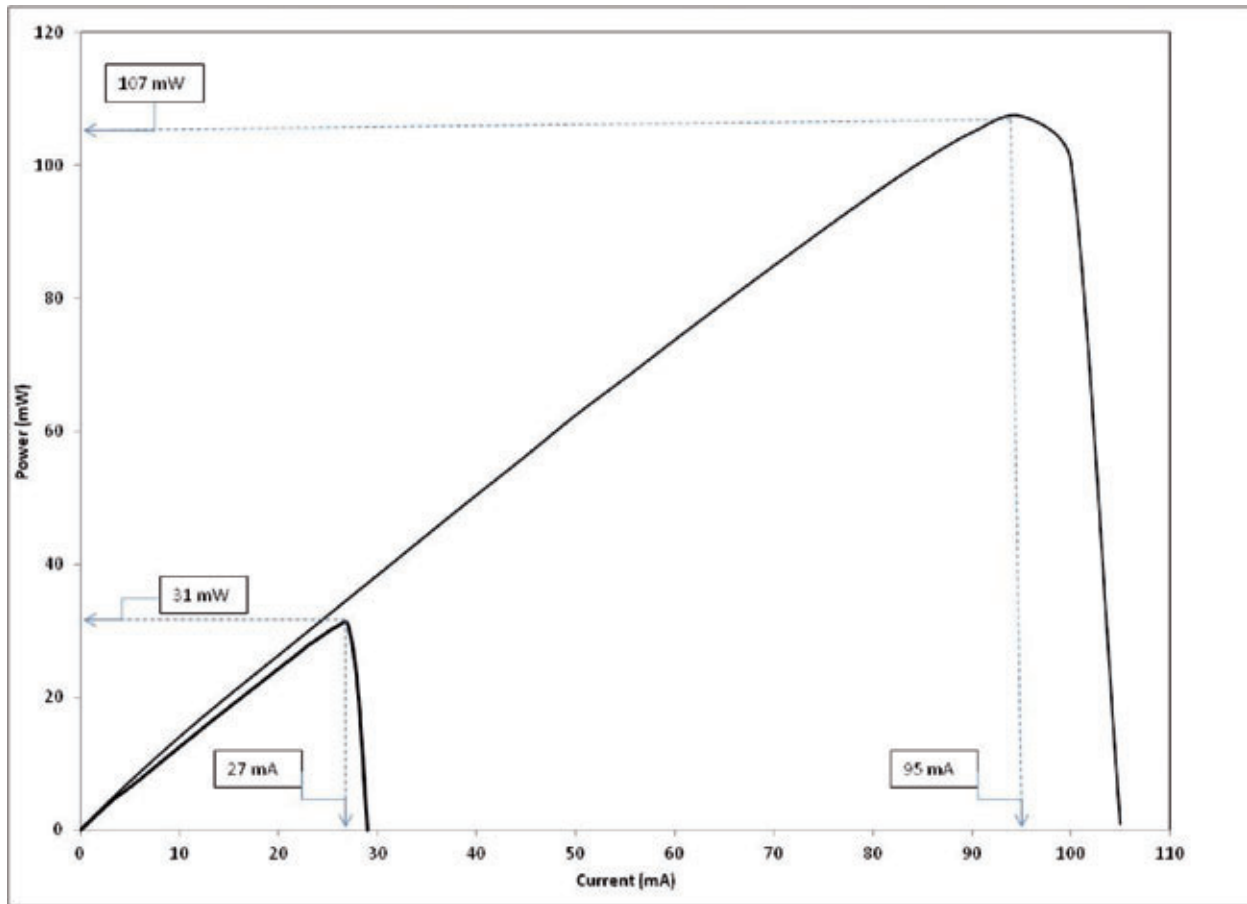


Figure 7. Power output profiles of monopolar and bipolar cell configurations.

TABLE 2. Discharge characteristics of monopolar Zn/MCM-41/air cell at various load currents.

Discharge Current (mA)	Discharge Duration (min)	Average Operating Voltage (V)	Discharge Capacity (mAh)	Total Energy Output (mWh)
10	148	1.24	24.7	30.5
15	76	1.23	18.9	23.1
20	104	1.23	34.5	42.5
30	29	1.20	14.7	17.6

Cell discharge capacity (C) is a measure of zinc active material utilization at a particular load current and calculated from the product of discharge current ( $I_d$ ) and discharge duration ( $t$ )

$$C = I_d t \tag{2}$$

Total energy output (Q) is obtained from the product of  $I_d$  and the area under the discharge plot (operating voltage vs. discharge duration)

$$Q = I_d A_n = I_d \int_{t_o}^{t_f} V_{op}(t) dt \tag{3}$$

where  $A_n$  is the area under the discharge plot,  $V_{op}(t)$  is the instantaneous operating voltage of the cell, and  $\Delta t = t_f - t_o$  is the discharge duration.  $A_n$  can be estimated using the Riemann's Sum approximation

$$A_n = \sum_{i=1}^n \Delta x f(c_i) \tag{4}$$

$n$  is the number of data points,  $\Delta x$  is the interval between data points, and  $f(c_i)$  is the mid-point value between data point  $i-1$  and  $i$  ( $i = 1,2,3,\dots$ ) i.e. the average cell potential value between successive data points.

Figure 8 illustrates the discharge performance comparison between the monopolar and bipolar cell designs, rated at 20 mA. The bipolar cell registered a discharge capacity of 87.5 mAh and possessed total energy output of 109.4 mWh, an improvement factor of 2.5 as compared to the monopolar cell. We further evaluated the bipolar cell discharge capability at higher load currents,

as displayed in Figure 9. Table 3 summarizes the discharge characteristics obtained from the bipolar cell. Oxygen reduction is the rate limiting reaction in metal-air system (Chakkaravarthy *et al.*, 1981). A bipolar cell design doubles the active surface area of the air electrode. As such, the cell high rate capability was improved substantially.

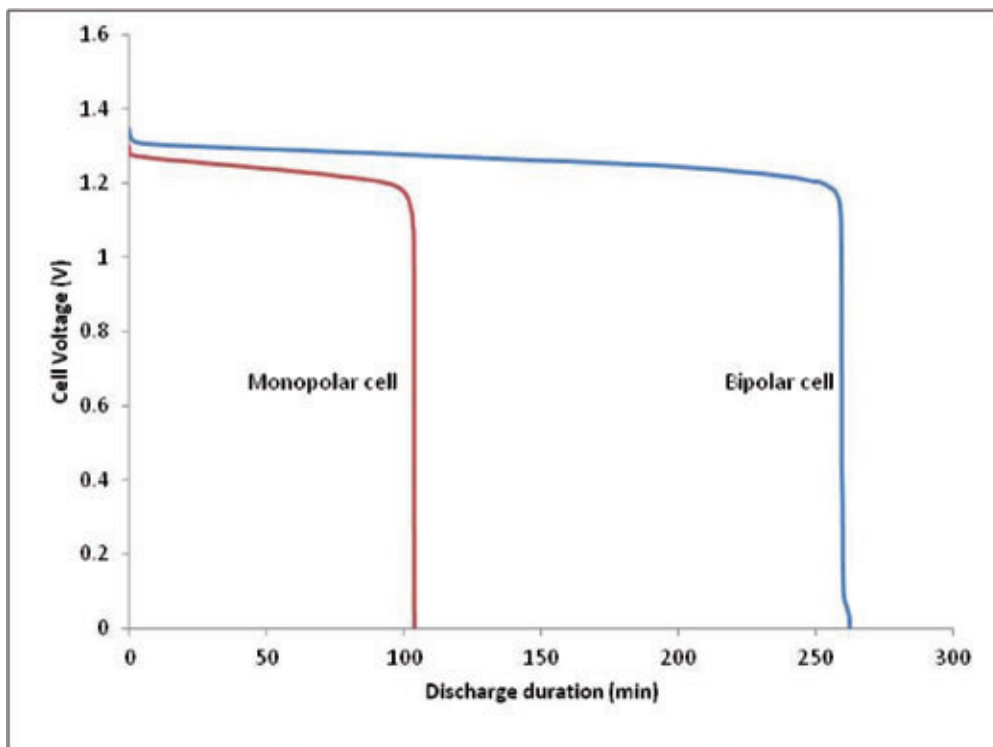


Figure 8. Discharge curves of monopolar and bipolar cell configurations rated at constant current of 20 mA

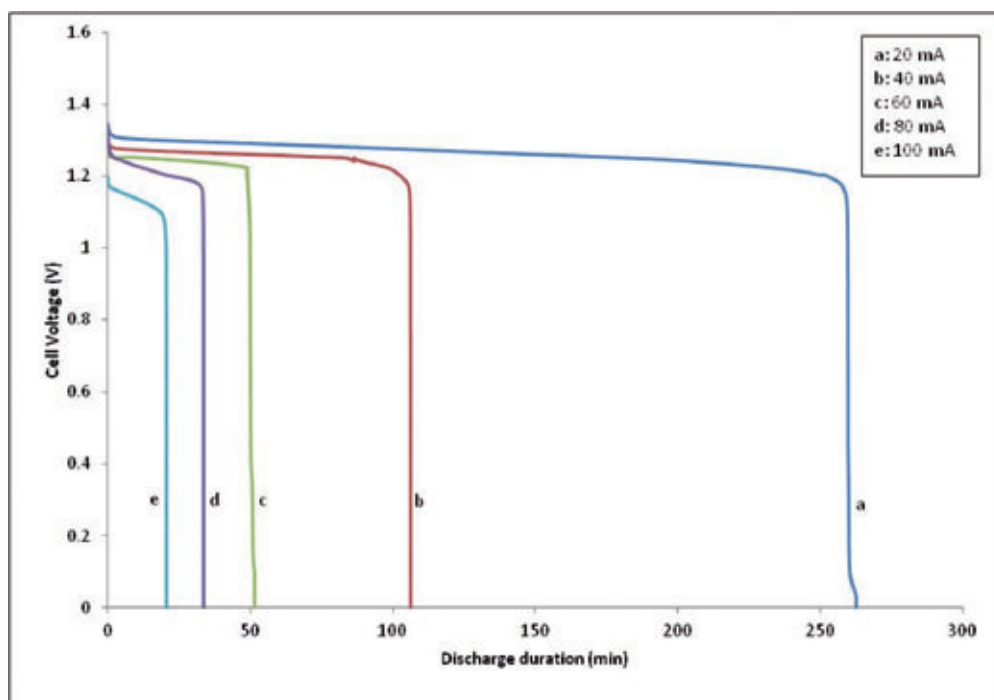


Figure 9. Discharge performance of bipolar cell rated at various load currents



**TABLE 3. Discharge characteristics of bipolar Zn/MCM-41/air cell at various load currents.**

Discharge Current (mA)	Discharge Duration (min)	Average Operating Voltage (V)	Discharge Capacity (mAh)	Total Energy Output (mWh)
20	260	1.26	87.5	109.4
40	106	1.25	70.0	89.0
60	50	1.24	51.7	62.5
80	33	1.21	44.6	54.1
100	21	1.13	34.6	39.1

The discharge characteristics obtained from the zinc/MCM-41/air monopolar cell are comparable to the published product datasheet for Duracell's zinc-air button cells as listed in *Table 4*. The limiting current and maximum power output are comparable even for button cell DA630 which is of larger size (15.57 mm diameter, 6.17 mm height). Although the rated capacity of the button cell is much higher, its volumetric size of 1.17 cm<sup>3</sup>

is almost 25 times bigger than the present cell's volume of ca. 0.05 cm<sup>3</sup> (1 cm<sup>2</sup> area size and 0.46 mm thick). In short, the zinc-air cell employing MCM-41 membrane as the separator material demonstrates equivalent performance to the commercial cell, if not better. The bipolar design further enhanced the cell discharge characteristics by more than twofold.

**TABLE 4. Characteristics of Duracell's zinc-air button cells (Bender et al., 1995).**

Cell Type	Dimensions Diameter (mm) x Height (mm)	Rated Capacity (mAh)	Limiting Current, I <sub>L</sub> (mA)	Maximum output I <sub>L</sub> x 1.1 V (mW)
DA230	5.84 x 3.56	50	2	2.2
DA312	7.80 x 3.50	110	7	7.7
DA13	7.80 x 5.33	210	12	13.2
DA675	11.56 x 5.33	520	22	24.2
DA630	15.57 x 6.17	1000	25	27.5
DA1204	30.56 x 10.72	6300	150	165

## Conclusion

A feasible, compact and high discharge rate zinc/MCM-41/air cell has been demonstrated. Zinc/MCM-41/air cell of monopolar design, measured 1 cm<sup>2</sup> area x ca. 460 μm thick and weighed 50 mg, possessed the following properties: open circuit voltage of 1.5 V, limiting current of 27 mA, maximum power output of 31 mW, and volumetric energy density of 924 Wh l<sup>-1</sup>, rated at 20 mA. A bipolar design further enhanced the cell performance; limiting current of 95 mA, maximum power output of 107 mW, and volumetric energy density of 1189 Wh l<sup>-1</sup>. These characteristics are in fact of comparable performance to commercial zinc-air cells. We attribute the high rate capacity of the cell to the use of inorganic MCM-41 separator material. The ultrathin membrane structure, high surface area and porous nature, and hydrophilic characteristics, are the key contributing factors.

## Acknowledgement

The work was funded by research grant awarded by the ISESCO Centre for Promotion of Scientific Research (ICPSR). The authors gratefully acknowledge the financial support.

## References

- [1] Backhurst, J.R., Goodridge, F., Plimley, R.E., and Fleischmann, M. (1996). Some aspects of a fluidized zinc-oxygen electrode system, *Nature*, 221, pp. 55-59
- [2] Beck J.S., Vartuli J.C., Roth W.J., Leonowicz M.E., Kresge C.T., Schmitt K.D., Chu C.T.D., Olson D.H., Sheppard E.W., McCullen S.B., Higgins J.B. and Schlenker J.L. (1992). A new family of mesoporous molecular sieves prepared with liquid crystal templates, *J. Am. Chem. Soc.*, 114, pp. 10834-10843
- [3] Bender, S. F., Cretzmeyer, J. W. and Reise, T. F. (1995). *Handbook of Batteries* (2<sup>nd</sup> Ed.), Linden, D. (Editor), McGraw-Hill (New York), Chapter 13
- [4] Chakkaravarthy, C., Abdul Waheed, A.K., and Udupa, H.V.K. (1981). Zinc-air alkaline batteries-A review, *J. Power Sources*, 6, pp. 203-228
- [5] Chen, J., Li, Q., Xu, R. and Xiao, F. (1996). Distinguishing the silanol groups in the mesoporous molecular sieve MCM-41, *Angewandte Chemie*, 34, pp. 2694-2696
- [6] Dewi, E.L., Oyaizu, K., Nishide, H., and Tsuchida, E. (2003). Cationic polysulfonium membrane as separator in zinc-air cell, *J. Power Sources*, 115, pp. 149-152
- [7] Ghiurcan, G.A., Liu, C.C., Webber, A., and Feddrix, F.H. (2003). Development and characterization of a thick-film printed zinc-alkaline battery, *J. Electrochem Soc*, 150, pp. A922-A927
- [8] Goldstein, J.R., Brown, I., and Koretz, B. (1999). New developments in the Electric Fuel Ltd. zinc/air system, *J. Power Sources*, 80, pp. 171-179
- [9] Jia L., Katiyara A., Pintoa N.G., Jaroniec M. and Smirniotis P.G. (2004). Al-MCM-41 sorbents for bovine serum albumin: Relation between Al content and performance, *Micropor. Mesopor. Mater.* 75, pp. 221
- [10] Jiricny, V., Siu, S., Roy, A., and Evans, J.W. (2000). Regeneration of zinc particles for zinc-air fuel cells in a spouted-bed electrode, *J. Appl. Electrochem*, 30, pp. 647-656
- [11] Lee Y.S. and Rathman J.F. (2001). *Reactions and Synthesis in Surfactant Systems*, Surfactant Science Series (Vol. 100), Texter J. (Editor), Marcel Dekker Inc., pp. 779-796
- [12] Kresge, C. T., Leonowicz, M. E., Roth, W. J., Vartuli, J. C. and Beck, J. S. (1992). Ordered mesoporous molecular sieves synthesized by a liquid-crystal template mechanism, *Nature*, 359, pp. 710-712
- [13] Muller, S., Haas, O., Schlatter, C., and Comminellis, C. (1998). Development of a 100 W rechargeable zinc/oxygen battery, *J. Appl. Electrochem.*, 28, pp. 305-310
- [14] Nor Hairin A.L., Othman R., Ani M.H. and Saputra H. (2011). High discharge rate electrodeposited zinc electrode for use in alkaline microbattery, *IJUM Eng. J.*, 12, pp. 115-122
- [15] Othman, R., Yahaya, A.H., and Arof, A.K. (2002). A zinc-air cell employing a porous zinc electrode fabricated from zinc-graphite-natural biodegradable polymer paste, *J. App. Electrochem.* 32, pp. 1347-1353
- [16] Øye, G., Sjöblom, J. & Stöcker, M. (2001). Synthesis, characterization and potential applications of new materials in the mesoporous range, *Adv. Colloid Interface Sci.*, 89, pp. 439-466.
- [17] Sano T., Kasuno T., Arazaki S. and Kawakami Y. (1997). Sorption of water vapor on HZSM-5 type zeolites, *Stud. Surf. Sci. Catal.*, 105, pp. 1771-1778
- [18] Saputra H. (2003). Synthesis and characterization of zirconium-containing nanoporous silica membranes, Master Thesis, Osaka University, Japan.
- [19] Saputra, H., Othman, R., Sutjipto, A. G. E., and Muhida, R. (2011). MCM-41 as a new separator material for electrochemical cell: Application in zinc-air system, *J. Mem. Sci.*, 367, pp. 152-157
- [20] Saputra, H., Othman, R., Sutjipto, A. G. E., and Muhida, R. (2011a). High energy density zinc-air microbattery utilising inorganic MCM-41 membrane, *Mater. Res. Innov.*, 15, pp. s114-s117
- [21] Saputra H., Othman R., Sutjipto A. G. E., Muhida R. and Ani M. H. (2012). Gel-like properties of MCM-41 material and its transformation to MCM-50 in a caustic alkaline surround, *Mat. Res. Bull.*, 47 pp. 732-736
- [22] Savaskan, G., Huh, T., and Evans, J.W. (1992). Further studies of a zinc-air cell employing a packed bed anode part I: Discharge, *J Appl Electrochem*, 22, pp. 909-915
- [23] Smee, A. (1840). On the galvanic properties of the metallic elementary bodies, with a description of a new chemico-mechanical battery, *Phil. Mag.* III, 16, pp. 315-321
- [24] Zhang, G.Q., and Zhang, X.G. (2004). MnO<sub>2</sub>/MCMB electrocatalyst for all solid-state alkaline zinc-air cells, *Electrochim. Acta*, Vol. 49, pp. 873-877
- [25] Zhao, X. S. and Lu, G. Q. (1998). Modification of MCM-41 by surface silylation with trimethylchlorosilane and adsorption study, *J. Phys. Chem. B*, 102, pp. 1556-1561